Magnetic properties of Mn-doped GaN with defects: *ab-initio* calculations

E. Salmani[a)], A. Benyoussef[a)], H. Ez-Zahraouy[a)†], and E. H. Saidi[b)]

[a)] *LMPHE, Departement de Physique, Faculté des Sciences, Université Mohammed V-Agdal, Rabat, Morocco*
[b)] *LPHE, Departement de Physique, Faculté des Sciences, Université Mohammed V-Agdal, Rabat, Morocco*

(Received 24 October 2010; revised manuscript received 19 April 2011)

According to first-principles density functional calculations, we have investigated the magnetic properties of Mn-doped GaN with defects, $Ga_{1-x-y}V_{Gx}Mn_y\ N_{1-z-t}V_{Nz}O_t$ with Mn substituted at Ga sites, nitrogen vacancies V_N, gallium vacancies V_G and oxygen substituted at nitrogen sites. The magnetic interaction in Mn-doped GaN favours the ferromagnetic coupling via the double exchange mechanism. The ground state is found to be well described by a model based on a Mn^{3+}–d^5 in a high spin state coupled via a double exchange to a partially delocalized hole accommodated in the 2p states of neighbouring nitrogen ions. The effect of defects on ferromagnetic coupling is investigated. It is found that in the presence of donor defects, such as oxygen substituted at nitrogen sites, nitrogen vacancy antiferromagnetic interactions appear, while in the case of Ga vacancies, the interactions remain ferromagnetic; in the case of acceptor defects like Mg and Zn codoping, ferromagnetism is stabilized. The formation energies of these defects are computed. Furthermore, the half-metallic behaviours appear in some studied compounds.

Keywords: diluted magnetic semiconductor, GaN:Mn, defects, *ab-initio,* magnetic properties

PACS: 66.30.Xj, 72.20.Dp, 72.20.My, 72.25.Dc **DOI:** 10.1088/1674-1056/20/8/086601

1. Introduction

Gallium nitride has attracted significant attention for various electronic and optoelectronic applications, such as light-emitting diodes (LEDs), blue laser diodes, high power and high frequency devices,[1−6] due to its superb electrical properties, high electron saturation velocity, direct wide band-gap, and high breakdown strength. In addition, GaN doped with magnetic impurities provides extra flexibility for spin-based electronic (spintronics) applications: magnetic random access memory and quantum computing.[7] Mn-doped GaN is a fairly suitable candidate for spintronic applications because of its promising room temperature ferromagnetism.[8]

However, the nonuniform distribution of the Mn component within (Ga, Mn)N layers has been reported to form micro-precipitates and clusters, having detrimental effects on the efficiency and quality of the material.[9,10] Many experimental studies have been carried to date.[11−20] However, the origin of experimentally observed ferromagnetism has still not been fully understood. The study of $Ga_{1-x}Mn_xN$ as thin films or nanocrystals exhibits ferromagnetism and a Curie temperature above room temperature and that p- or n-type doping of $Ga_{1-x}Mn_xN$ can change its magnetic state.

It was predicted theoretically that the ferromagnetic (FM) interaction in (Ga, Mn)N may be retained up to room temperature.[8] The initial reports of high T_C in (Ga, Mn)N were followed by controversial results where the reported T_c varied between 20 K and 940 K.[21−23] Zajac *et al.*[24] observed that Mn ions in $Ga_{1-x}Mn_xN$ ($x < 0.1$) crystals are coupled anti-ferromagnetically (AFM). Electronic structures and magnetic properties of zinc blende $Ga_{1-x}Mn_xN$ for several values of x with varied spatial distribution of dopant atoms to understand the magnetic interaction for an explanation of FM–AFM competition was discussed by Uspenskii *et al.*,[25] where the calculations were done using the tight binding LMTO (Linear Muffin-Tin Orbital Method) method in the local spin density approximation. Sanyal and Mirbt[26] studied Mn-doped GaAs and GaN DMS using the *ab-initio* plane wave code (VASP) within the frame of density functional theory (DFT). They determined the interatomic exchange interactions by substituting Mn in various positions in the unit cell and attributed the ferromagnetism in (Ga, Mn)N to a double-exchange mechanism involving the hopping of Mn–d electrons. Raebiger *et al.*[27] used the full po-

†Corresponding author. E-mail: ezahamid@fsr.ac.ma

© 2011 Chinese Physical Society and IOP Publishing Ltd

tential linearized augmented plane wave (FP-LAPW) method to investigate the interplay between clustering and exchange coupling in the magnetic semiconductor $Ga_{1-x}Mn_xAs$. They studied all possible arrangements of the two Mn atoms on a Ga sublattice for $x \sim 5\%$ and found that clustering of Mn atoms at near neighbour Ga sites is energetically preferred.

The aim of this paper is to consider the role of defects in promoting ferromagnetism. Here we report on the results of density functional theory (DFT) calculations of the electronic states induced by defects (N vacancy, $V_{\rm N}$, Ga vacancy, $V_{\rm Ga}$, and O substituted for N, O_N) as well as the electronic structures of bulk GaN and $Ga_{1-x}Mn_xN$ with different values of x.

2. Calculation methods

The band structures of Wurtzite $Ga_{1-x}Mn_xN$ ($x = 0.05$) were investigated using the Korringa–Kohn–Rostoker method combined with the coherent potential approximation (KKR–CPA), with the parameterization of Moruzzi, Janak and Williams (MJW), and Vosko, Wilk, and Nusair (VWN).[28] The MJW and VWN functionals predict a band gap of approximately 2.72 eV for bulk GaN, comparable to the experimental value of 3.507 eV. We supposed that Ga atoms were replaced by magnetic impurities randomly. The KKR–CPA is one of the most sophisticated methods of treating such substitutional disordered systems while taking disorder into account in an *ab initio* manner. Akai and Dederichs have developed the KKR–CPA method to treat transition metal alloys[29] and InAs-based DMS,[30] and explained their magnetic properties successfully. Sato and Katayama-Yoshida proposed a material design for transparent ferromagnets with ZnO-based DMSs using the KKR–CPA.[31,32] For the principles of the KKR–CPA, see Refs. [29] and [30].

The form of the crystal potential is approximated by a muffin-tin potential, and the wave functions in the respective muffin-tin spheres were expanded in real harmonics up to $l = 2$, where l is the angular momentum quantum number defined at each site. We use higher K-points up to 250 in the irreducible part of the first Brillouin zone. In the present calculations, we used the KKR–CPA code MACHIKANEYAMA2002v08 package produced by Akai.[33] In GaN crystal, each atom of gallium is surrounded by four cations of nitrogen on the corners of a tetrahedron and *vice versa*. This tetrahedral coordination is typical of sp^3 covalent bonding but do not forget that these materials also each have a substantial ionic characteristic. This crystalline structure is known as wurtzite structure and has a hexagonal unit cell with two lattice parameters. GaN has the wurtzite crystal structure and its lattice constants are $a = 3.180$ Å (1 Å=0.1 nm), and $c = 5.166$ Å. The internal coordinate u for the GaN wurzite structure is $u = 0.377$.[34]

3. Results and discussion

3.1. Magnetic interaction in Mn-doped GaN

Total and partial densities of states of $Ga_{1-x}Mn_xN$ ($x = 0.05$) are presented in Fig. 1(a). The upper curves refer to the majority density of state (DOS), and the lower inverted ones to the minority DOS. The band structure of zinc-blende $Ga_{1-x}Mn_xN$ ($x = 0.05$) in the ferromagnetic state is shown in Figs. 1(b) and 1(c) for spin up and spin down, respectively. The 3d bands of Mn with spin up are very narrow and they are situated in the gap. These bands are not hybridized with the valence band and the 3d-orbitals are localized near Mn atoms.

Due to the low concentration of Mn, this is roughly the DOS of the pure semiconductors, consisting of the occupied valence band, dominated by the anion p-states and the empty conduction band, formed mostly by the Ga s-states. Since Mn has 7 valence electrons and substitutes for a Ga atom, 3 of the 7 electrons can replace the 3 Ga electrons in the valence band. The remaining 4 electrons have to be located in new localized d-states in the band gap. Therefore the electronic structure of transition metal impurity in semiconductor is dominated by d-states in the gap, which for finite concentrations develop into an impurity band. Thus the 3d-states of Mn are situated in the gap of (Ga, Mn)N. The 3d-states of Mn are split by exchange interaction between 3d-electrons of Mn: the 3d-states of Mn with spin up each have a lower energy than the 3d-states with spin down. This relative position of 3d-states ensures the maximal total spin moment when the population of the 3d-states increases, which is consistent with Hund's rule for free atoms. The size of the exchange splitting is of (~ 2 eV), consistent with the previous study by Sato

and Katayama-Yoshida[35] and with experimental results (∼ 1.8 eV) obtained in Ref. [36]. The crystal field caused by the four nearest-neighbour N atoms additionally splits the 3d-states of Mn into a doubly degenerate e band and a triply degenerate t_a band. The t_a band consists of d-orbitals that have xy, yz, and xz symmetries, while the e band is composed of 3d-orbitals that have x^2–y^2 and $2z^2$–x^2–y^2 symmetries. Geometrically, the $d(xy, yz, xz)$-orbitals are closer to the nearest-neighbour N atoms than $d(x^2$–y^2, $2z^2$–x^2–$y^2)$-orbitals of Mn. The strong interaction of the 3d(t_a) states of Mn with the 2p states of N splits the t_2 band into bonding (∼ 2 eV) and anti-bonding (above −1 eV) parts and pushes up the anti-bonding part of the d(t_2) band above the d(e) band, consistent with

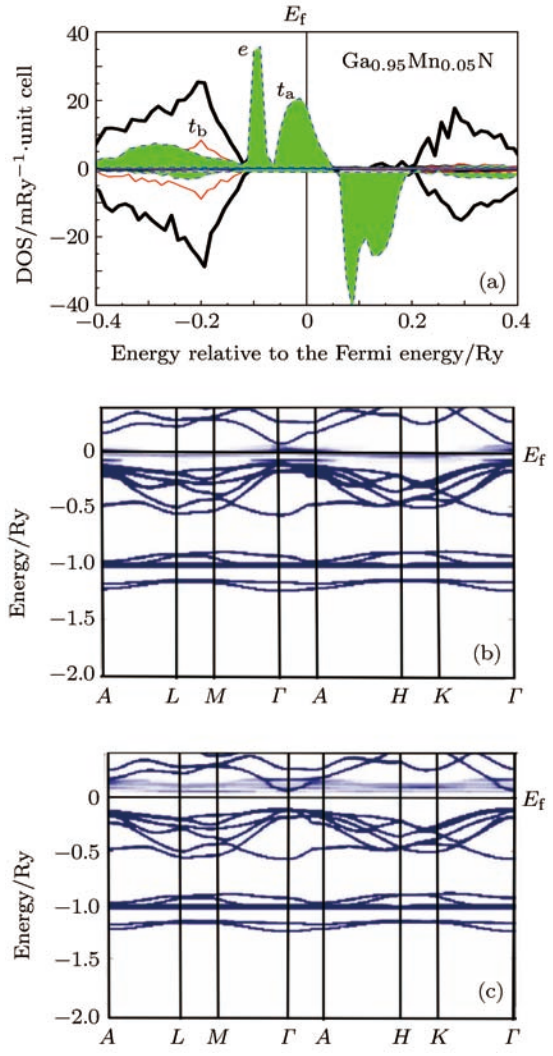


Fig. 1. (a) Total d and p state projected densities of state (DOSs) of Mn, doped GaN, $Ga_{1-x}Mn_xN$, with $x = 0.05$. The total DOS is denoted by a thick solid line, 3d-states of Mn by a filled area, 2p-states of N by a thin solid line; (b) band structure of up spin, doped GaN, $Ga_{1-x}Mn_xN$, with $x = 0.05$; (c) band structure of down spin, doped GaN, $Ga_{1-x}Mn_xN$, with $x = 0.05$ (1 Ry=13.605 eV).

the results obtained by Sato *et al.*[31,32] As a result, the 3d (e, spin up) band is filled by electrons, while the 3d(t_a, spin up) is partially empty. The ferromagnetic state is stabilized if there are carriers in itinerant t_a state. These itinerant electrons in t_a state participate in the double exchange mechanism to lower the kinetic energy of the ferromagnetic state. On the other hand, electrons in e state are rather localized and do not take part in the double exchange mechanism. Moreover, the ferromagnetic coupling appears with a small width of the anti-banding t_a state, which is not filled up completely (Fig. 1(a)). Increasing the concentration, the t_a width becomes larger, which indicates that the coupling is a ferromagnetic double exchange. Figures 1(a)–1(c) each also show a half-metallic behaviour, which is reinforced by increasing the impurity concentration of Mn. Indeed, the calculated total magnetic moment for $Ga_{1-x}Mn_xN$ increases from 0.167 μ_B to 0.405 μ_B with the impurity concentration (x) increasing from 0.02 to 0.05, respectively. It is obvious that the greatest contribution of this magnetization comes from Mn for which the partial magnetic moments are 3.132 μ_B and 3.073 μ_B for $x = 0.02$ and $x = 0.05$, respectively. In addition, the weak partial magnetic moments appearing for nitrogen are 0.004 μ_B for $x = 0.02$ and 0.008 μ_B for $x = 0.05$.

3.2. Influence of defects

Early experimental work reported by several groups did not give any clear conclusion about the magnetic properties of (Ga, Mn)N: paramagnetic[21] and ferromagnetic properties at low temperature (T_C ∼ 10 K and 8 K),[37] as well as room temperature ferromagnetism in (Ga, Mn)N. The highest Curie temperature (T_C ∼ 940 K) was deduced from magnetization measurements of (Ga, Mn)N layers.[38] Such a variety of contradictory results can be explained by different types of distribution of Mn impurity and additional defects in different (Ga, Mn)N samples. The Curie temperature may change upon co-doping with a donor or an acceptor. Therefore, the presence of unexpected impurities in (Ga, Mn)N samples may change the magnetic ground state.

3.2.1. Co-doping with a donor

In (Ga, Mn)N, the exchange interactions between Mn impurities appear via the double exchange mechanism proposed by Zener for the manganese compounds

with perovskite structure. This exchange mechanism leads to ferromagnetic order in compounds where equivalent Mn atoms have different valence states. In (Ga, Mn)N, this situation could be achieved by co-doping with a donor: one part of the Mn ions captures additional electrons and becomes Mn^{2+}, while the other part rests in the 3^+ valence state. According to the Zener's double-exchange mechanism, the additional electrons can move from Mn^{2+} to Mn^{3+} ions and these electron jumps reduce the total energy of the crystal. It is assumed that the oscillations are possible only when the spins of the Mn ions are parallel. If spin moments of neighbouring Mn atoms are antiparallel, then such oscillations of electrons are forbidden because the spin moment should not change direction. Therefore the (Ga, Mn)N crystals should be ferromagnetic if a mixture of Mn^{3+} and Mn^{2+} ions is present in the crystals. However, the calculations we performed using the KKR-CPA method show that the co-doping with donors does not always stabilize the ferromagnetism. In fact, spin glass ground states are predicted for co-doping (Ga, Mn)N by a donor such as oxygen substituted at nitrogen sites and nitrogen vacancies, $Ga_{1-y}Mn_yN_{1-z-t}O_tV_{Nz}$, because t_a state is full and (Ga, Mn)N remains of n type, as shown in Fig. 2. In this case, the exchange coupling between Mn impurities is an antiferromagnetic super-exchange.

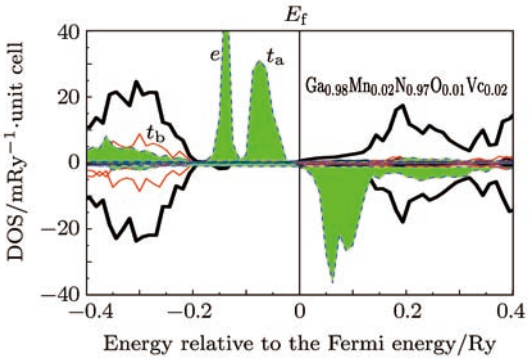


Fig. 2. Total d and p state projected densities of state of $Ga_{0.98}Mn_{0.02}N_{0.97}O_{0.01}Vc_{0.02}$. The total DOS is denoted by a thick solid line, 3d-states of Mn by a filled area, and 2p-states of O and N by a thin solid line.

However, weak magnetism is obtained for the co-doping with a donor such as Ga vacancies, $(Ga_xV_{G(1-x)})_yMn_{(1-y)}N$, which is shown in Fig. 3, where the total moment is ~ 0.084 μ_B and a hybridization between Mn-3d and N-2p is observed at Fermi energy, with the partial magnetic moments 2 μ_B and -0.008 μ_B, respectively. One observes a decrease in the Mn moment in comparison with the $Ga_{1-x}Mn_xN$ case. We note also that the half metallicity disappears with donor co-doping. These results are in accordance with experimental investigations, which show that the electronic state of Mn changes under donor co-doping: Mn ions capture the extra electrons and become $Mn2^+$.[39] As shown previously, the 3d states of $Mn3^+$ are localized near Mn ions and do not contribute to electrical conductivity. An experimental demonstration of this statement can be found in Ref. [40], where the 3^+ valence state of Mn was found in $Ga_{1-x-y}Mn_xMg_yN$ samples and the samples were insulating.

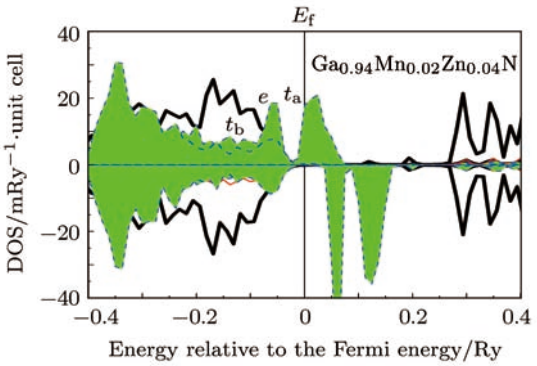


Fig. 3. Total d and p states projected of Mn, doped GaN, $Ga_{0.94}Mn_{0.02}Zn_{0.04}N$. The total DOS is denoted by a thick solid line, 3d-states of Mn and Zn by a filled area, and 2p-states of N by a thin solid line.

3.2.2. Co-doping with an acceptor

Co-doping with an acceptor, like free holes, can mediate exchange interactions between impurity atoms. However, there is no efficient acceptor today to create a very high concentration of holes, especially if double co-doping must be performed (with Mn and Mg). Shon *et al.*[41] have observed experimentally that the transition point related to the GaMnN DMS phase for p-type Mg-codoped GaMnN was higher than that of undoped GaMnN. This is due to the increase in ferromagnetic interaction rates governed by the co-doping of Mg acceptors.

In this section, we study the effect of acceptor co-doping considering $(Ga_xMg_{(1-x-u)}Zn_u)_yMn_{(1-y)}N_{1-z}O_z$ and $(Ga_xMg_{(1-x-u)}Zn_u)_yMn_{(1-y)}N_{1-z}Vc_z$. The use of both undoped and p-type GaN at the same time was based on the motivation that we intend to estimate the origin and the variation in magnetic properties due to the effect of holes after Mn-doping. In the absence of oxygen and vacancy sites ($Ga_{0.94}Zn_{0.04}Mn_{0.02}N$), the half metallic behaviour is observed (Fig. 4(a)); the majority-spin t_a states are

located at the Fermi level, while the majority-spin e states are on the valence band edge.

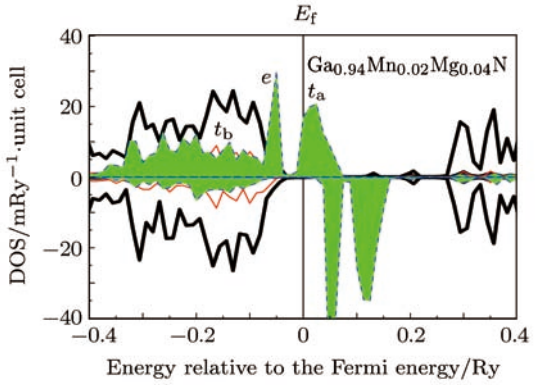


Fig. 4. Total d and p state projected densities of state of $Ga_{0.94}Mn_{0.02}Mg_{0.04}N$. The total DOS is denoted by a thick solid line, 3d-states of Mn by a filled area, and 2p-states of N and Mg by a thin solid line.

Furthermore, the ferromagnetism is stabilized due to double exchange coupling. The stability of the ferromagnetic phases has been computed by comparing the total energies of ferromagnetic and antiferromagnetic configurations, as given in Table 1. However, the total magnetic moment is weak around 0.1, while the partial moments of Mn, Zn, and N are 2.353 μ_B, -0.005 μ_B, and -0.004 μ_B, respectively. Indeed, experimental studies of the electronic states of (Ga, Mn)N co-doped with Mg showed that the Mg addition stabilizes the $Mn4^+$ charge state by reducing the Fermi level.[42]

Table 1. Differences in total energy between ferromagnetic and antiferromagnetic configurations for different compounds.

Compound	$(\Delta_{AFM} - \Delta_{FM})$/Ry
$Ga_{0.98}Mn_{0.02}N$	0.1257
$Ga_{0.95}Mn_{0.05}N$	0.2290
$Ga_{0.96}Mn_{0.02}Vc_{0.02}N$	0.0169
$Ga_{0.94}Mn_{0.02}Zn_{0.04}N$	0.4848
$Ga_{0.94}Mn_{0.02}Zn_{0.04}N_{0.98}Vc_{0.02}$	0.1745
$Ga_{0.94}Mn_{0.02}Zn_{0.04}N_{0.98}O_{0.02}$	0.1173
$Ga_{0.94}Mn_{0.02}Mg_{0.04}N$	0.3521
$Ga_{0.94}Mn_{0.02}Mg_{0.02}Zn_{0.02}N$	0.3919
$Ga_{0.94}Mn_{0.02}Mg_{0.02}Zn_{0.02}N_{0.99}O_{0.01}$	0.3914

In the case of Mg co-doping ($Ga_{0.94}Mg_{0.04}Mn_{0.02}N$) (Fig. 4(b)), the ferromagnetism is also stabilized, with a less strong half metallic behaviour. However, there are no significant changes in magnetic moments; 2.249 μ_B and -0.005 μ_B, for Mn and N, respectively.

For low oxygen concentration $Ga_{0.94}Zn_{0.04}Mn_{0.02}N_{0.98}O_{0.02}$ and $Ga_{0.94}Mg_{0.04}Mn_{0.02}N_{0.98}O_{0.02}$ (Figs. 5(a) and 5(b)) or vacancy sites $Ga_{0.94}Zn_{0.04}Mn_{0.02}$ $N_{0.98}$ $Vc_{0.02}$ (Fig. 6) the half metallic behaviour is enhanced, and the ferromagnetism is still stabilized by double exchange coupling, with total magnetic moments being 0.132 μ_B, 0.167 μ_B, and 0.132 μ_B, respectively.

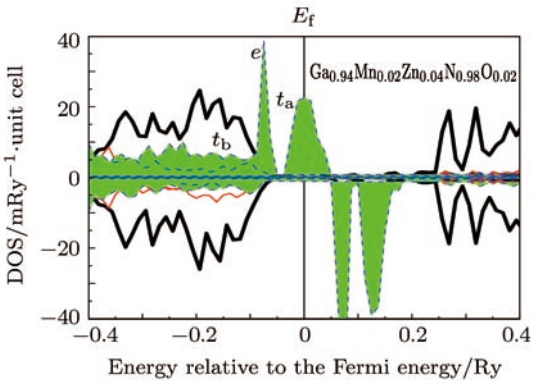


Fig. 5. Total d and p states projected densities of state of $Ga_{0.94}Mn_{0.02}Zn_{0.04}N_{0.98}O_{0.02}$. The total DOS is denoted by a thick solid line, 3d-states of Mn and Zn by a filled area, and 2p-states of N by a thin solid line.

3.3. Heats of formation

In order to study the stabilities of these compounds, we calculate the heat of formation Δ_{EHF}, which is defined in the first step as a difference in total energy between doped compound $Ga_{1-x}Mn_xN$ and GaN, and in the second step as a difference in total energy between the co-doped compound $(Ga_xMg_{(1-x-u)}Zn_u)_yMn_{(1-y)}N_{1-z}O_z$ or $(Ga_xMg_{(1-x-u)}Zn_u)_yMn_{(1-y)}N_{1-z}Vc_z$ and the doped compound $Ga_{1-x}Mn_xN$. The heats of formation of the studied compounds are listed in Table 2. It is worthwhile noting that $Ga_{1-x}Mn_xN$ is less stable than GaN (Δ_{EHF} = 49.490899 Ry, 1 Ry=13.605 eV), and $Ga_xMg_{(1-x-u)}Zn_u)_yMn_{(1-y)}N_{1-z}O_z$ and $(Ga_xMg_{(1-x-u)}Zn_u)_yMn_{(1-y)}N_{1-z}Vc_z$ are found to be less stable than $Ga_{1-x}Mn_xN$, except for $Ga_{0.98}Mn_{0.02}N_{0.95}O_{0.05}$, which is more stable ($\Delta_{EHF}$ = -4.113294 Ry). However, the substitution of N with oxygen and vacancy, $Ga_{0.98}Mn_{0.02}N_{0.97}O_{0.01}Vc_{0.02}$, has a weak formation energy (Δ_{EHF} = 3.5451989 Ry). The co-doping with Zn needs relatively higher energy, Δ_{EHF} = 23.2569545 Ry, for $Ga_{0.94}Mn_{0.02}Zn_{0.04}N$. While, co-doping with Mg is high, Δ_{EHF} = 275.6469894 Ry, for $Ga_{0.94}Mn_{0.02}Mg_{0.04}N$.

Table 2. Heat of formation of the compounds under study.

Compound	$\Delta_{\rm EHF} = [E(\text{compound}) - E(Ga_{0.98}Mn_{0.02}N)]/\text{Ry}$
GaN	–49.490899
$Ga_{0.96}Mn_{0.02}Vc_{0.02}N$	153.9164154
$Ga_{0.98}Mn_{0.02}N_{0.95}O_{0.05}$	–4.113294
$Ga_{0.98}Mn_{0.02}N_{0.98}O_{0.01}Vc_{0.02}$	3.5451989
$Ga_{0.94}Mn_{0.02}Zn_{0.04}N$	23.2569545
$Ga_{0.94}Mn_{0.02}Zn_{0.04}N_{0.98}O_{0.02}$	21.6251126
$Ga_{0.94}Mn_{0.02}Zn_{0.04}N_{0.98}Vc_{0.02}$	27.6346286
$Ga_{0.94}Mn_{0.02}Mg_{0.04}N$	275.6469894
$Ga_{0.94}Mn_{0.02}Mg_{0.04}N_{0.96}O_{0.04}$	272.3778483
$Ga_{0.94}Mn_{0.02}Mg_{0.02}Zn_{0.02}N$	149.4526694
$Ga_{0.94}Mn_{0.02}Mg_{0.02}Zn_{0.02}N_{0.98}O_{0.02}$	147.81969

4. Summary

In this paper, the magnetism of Mn-doped GaN and co-doping (Ga, Mn)N is investigated in detail by *ab initio* electronic structure calculations by using the KKR–CPA method. According to the present calculations, ferromagnetic DMSs are readily achievable in Mn-doped GaN-based DMSs and spin glass ground states are predicted for co-doping (Ga, Mn)N by a donor such as oxygen. The effect of defects on ferromagnetic coupling is investigated. It is found that in the presence of donor defects, such as oxygen substituted at nitrogen sites, nitrogen vacancy antiferromagnetic interactions appear while in the case of Ga vacancies, the interactions remain ferromagnetic, whereas in the case of acceptor defects like Mg and Zn codoping, ferromagnetism is stabilized.

Acknowledgment

We thank professor Hisazumi Akai for fruitful discussions and for providing us with his KKR–CPA band structure calculation package (MACHIKANEYAMA-2000). LMPHE: "Unité de Recherche Associée au CNRST (URAC)"

References

[1] Nakamura S 1998 in *GaN I, Semiconductors and Semimetals* ed. Pankov J N and Moustakas T D (New York: Academic) pp. 431–437
[2] Gil B 1998 *Group III Nitride Semiconductor Compounds: 'Physics and Applications'* (Oxford: Clarendon)
[3] Strite S and Marc_oc H 1992 *J. Vac. Sci. Technol.* B **10** 1237
[4] Nakamura S and Fasol G 1998 *The Blue Laser Diode* (Berlin: Springer)
[5] Orton J and Foxon C 1998 *Rep. Prog. Phys.* **61** 1
[6] Kung P and Razeghi M 2000 *Opt. Electron. Rev.* **8** 201
[7] Das Sharma S 2001 *Am. Sci.* **89** 516
[8] Dietl T, Ohno H, Matsukura F and Ferrand D 2000 *Science* **287** 1019
[9] Hasuike N, Fukumura H, Harima H, Kisoda K, Hashimoto M, Zhou Y K and Asahi H 2004 *J. Phys.: Condens. Matter* **16** S5811
[10] Harima 2004 *J. Phys.: Condens. Matter* **16** S5653
[11] Zajac M, Doradzinski R, Gosk J, Szczytko J, Lefeld M, Kaminska M, Twardowski A, Palczewska M, Granka E and Gebicki W 2001 *Appl. Phys. Lett.* **78** 1276
[12] Thaler G T, Overberg M E, Gila B P, Franzier R, Abernathy C R, Pearton S J, Lee J S, Lee S M, Park Y D, Khim Z G, Kim J and Ren F 2002 *Appl. Phys. Lett.* **80** 3964
[13] Shon Y, Kwon Y H, Yuldashev Sh U, Lim J H, Park C S, Fu D J, Kim H J, Kang T W and Fan X J 2002 *Appl. Phys. Lett.* **81** 1845
[14] Sonoda S, Shimizu S, Sasaki T, Yamamoto Y, Hori H and Cryst J 2002 *Growth* **237–239** 1358
[15] Ando K 2003 *Appl. Phys. Lett.* **82** 100
[16] Kim J, Ren F, Thaler G T, Frazier R, Abernathy C R, Pearton S J, Zavada J M and Whilson R G 2003 *Appl. Phys. Lett.* **82** 1565
[17] Marques M, Teles L K, Scolfaro L M R, Furthmüller J, Bechstedt F and Ferreira L G 2005 *Appl. Phys. Lett.* **86** 164105
[18] Baik J M, Shon Y, Kang T W and Lee J L 2005 *Appl. Phys. Lett.* **87** 42105
[19] Norton D P, Pearton S J, Hebard A F, Theodoropoulou N, Boatner L A and Wilson R G 2003 *Appl. Phys. Lett.* **82** 239
[20] Lee S, Shon Y, Lee S W, Hwang S J, Lee H S, Kang T W and Kim D Y 2006 *Appl. Phys. Lett.* **88** 212513
[21] Reed M L, El-Masry N A, Stadelmaier H H, Ritums M K, Reed M J, Parker C A, Roberts J C and Bedair S M 2001 *Appl. Phys. Lett.* **79** 3473
[22] Thaler G T, Overberg M E, Gila B, Frazier R, Abernathy C R, Pearton S J, Lee J S, Lee S Y, Park Y D, Khim Z G, Kim J and Ren F 2002 *Appl. Phys. Lett.* **80** 3964
[23] Ando K 2003 *Appl. Phys. Lett.* **82** 100
[24] Zajac M, Gosk J, Kaminska M, Twardowski A, Szyszko T and Podsiadlo S 2001 *Appl. Phys. Lett.* **79** 2432

[25] Uspenskii Y, Kulatov E, Mariette H, Nakayama H and Ohta H 2003 *J. Magn. Magn. Mater.* **258–259** 248

[26] Sanyal B and Mirbt S 2005 *J. Magn. Magn. Mater.* **290–291** 1408

[27] Raibiger H, Ayuela A and Nieminen R M 2004 *J. Phys.: Condens. Matter* **16** L457

[28] Vosko S H, Wilk L and Nusair M 1980 *Can. J. Phys.* **58** 1200

[29] Akai H and Dederichs P H 1993 *Phys. Rev.* B **47** 8739

[30] Akai H 1998 *Phys. Rev. Lett.* **81** 3002

[31] Sato K and Katayama-Yoshida H 2000 *Jpn. J. Appl. Phys.* **39** L555

[32] Sato K and Katayama-Yoshida H 2001 *Jpn. J. Appl. Phys.* **40** L334

[33] MACHIKANEYAMA2002v08: Akai H, Department of Physics, Graduate School of Science, Osaka University, Machikaneyama 1-1, Toyonaka 560-0043, Japan, akai@phys.sci.osaka-u.ac.jp

[34] Yeo Y C, Chong T C and Li M F 1998 *J. Appl. Phys.* **83** 1429

[35] Sato K, Schweika W, Dederichs P H and Katayama-Yoshida H 2004 *Phys. Rev.* B **70** 201202R

[36] Titov A, Biquard X, Halley D, Kuroda S, Bellet-Amalric E, Mariette H, Cibert J, Merad A E, Merad G, Kanoun M B, Kulatov E and Uspenskii Yu A 2005 *Phys. Rev.* B **72** 115209

[37] Jungwirth T, Wang K Y, Mašek J, Edmonds K W, König J, Sinova J, Polini M, Goncharuk N, MacDonald A H, Sawicki M, Rushforth A W, Campion R P, Zhao L X, Foxon C T and Gallagher B L 2005 *Phys. Rev.* B **72** 165204

[38] Kulatov E, Uspenskii Y, Mariette H, Cibert J, Ferrand D, Nakayama H and Ohta H 2003 *J. Supercond.* **16** 123

[39] Graf T, Gjukic M, Brandt M S, Stutzmann M and Ambacher O 2002 *Appl. Phys. Lett.* **81** 5159

[40] Wolos A, Wysmolek A, Kaminska M, Twardowski A, Bockowski M, Grzegory I, Porowski S and Potemski M 2004 *Phys. Rev.* B **70** 245202

[41] Jaeger C, Bihler C, Vallaitis T, Goennenwein S T B, Opel M, Gross R and Brandt M S 2006 *Phys. Rev.* B **74** 045330

[42] Han B, Wessels B W and Ulme M P 2005 *Appl. Phys. Lett.* **86** 042505